Chinese Journal of Polymer Science Vol. 35, No. 12, (2017), 1497–1507

Chinese Journal of Polymer Science
© Chinese Chemical Society
Institute of Chemistry, CAS
Springer-Verlag GmbH Germany 2017

Preparation of Nylon MXD6/EG/CNTs Ternary Composites with Excellent Thermal Conductivity and Electromagnetic Interference Shielding Effectiveness*

Yi-lan Guo, Run-zhi Zhang, Kai Wu, Feng Chen** and Qiang Fu**

College of Polymer Science and Engineering, State Key Laboratory of Polymer Materials Engineering, Sichuan University, Chengdu 610065, China

Abstract In this article, hybrid fillers with different dimensions, namely, 2-dimensional (2-D) expanded graphite (EG) and 1-dimensional (1-D) multi-walled carbon nanotubes (CNTs), were added to aromatic nylon MXD6 matrix *via* melt-blending, to enhance its thermal and electrical conductivity as well as electromagnetic interference shielding effectiveness (EMI SE). For ternary composites of MXD6/EG/CNTs, the electrical conductivity reaches up nine orders of magnitude higher compared to that of the neat MXD6 sample, which turned the polymer-based composites from an insulator to a conductor, and the thermal conductivity has been enhanced by 477% compared with that of neat MXD6 sample. Meanwhile, the EMI SE of ternary composite reaches ~50 dB at the overall filler loading of only 18 wt%. This work can provide guidance for the preparation of polymer composites with excellent thermal and electrical conductivity *via* using hybrid filler.

Keywords Thermal and electrical conductivity; Electromagnetic interference shielding; Hybrid filler; Synergistic effect

INTRODUCTION

Nowadays, accompanied by the fast development of polymer industry, the demand for multi-functional materials has reached a significant level. Present researchers have inclination towards some types of materials with excellent thermal and electrical conductivity, and at the same time, electromagnetic interference shielding effectiveness is one of the present research focuses as well. It is reported that the conductive composites not only exhibit excellent electrical conductivity but also have some feasibility in electromagnetic interference shielding due to the fact that in the presence of electromagnetic wave, materials with excellent electrical conductivity will generate a large amount of introduced current, which weakens the permeated radiation according to Lenz's law[1, 2].

It is also known that the traditional conductive materials include metals and ceramics. However, neither of them is ideal enough in the field of application as a result of their poor corrosion resistance and processability. On the other hand, polymer-based composites, with the advantages such as light weight, corrosion resistance and ease of processing, have received a wide spread attention over the academic field, as the properties of polymer materials are heavily dependent on the molecular weight[3], the introduction of a second component[4] or the addition of fillers with outstanding performance[5]. Since most polymers are neither thermal nor electrical conductors[6, 7], researchers have mostly focused on the incorporation of conductive fillers in polymer matrix, by

* This work was financially supported by the National Natural Science Foundation of China (Nos. 21274095 and 51573102).
** Corresponding authors: Feng Chen (陈枫), E-mail: fengchen@scu.edu.cn
Qiang Fu (傅强), E-mail: qiangfu@scu.edu.cn
Received April 13, 2017; Revised May 15, 2017; Accepted May 26, 2017
doi: 10.1007/s10118-017-1985-7

which conductive composites can be prepared with the combination of advantages from both polymer matrix and conductive fillers. Zeng *et al.* prepared PMMA/graphene electrical conductive composites by solution blending, then found that the electrical conductivity of composites reached up to 0.037 S/m even with only 2.0 wt% reduced graphene oxide (rGO), which was increased by more than twelve orders of magnitude[8]. Tu *et al.* used mechanical blending to make PE/multilayer graphite thermal conductive composites, and found the thermal conductivity reached 1.806 W/(m·K) for 50 wt% of the multilayer graphite loading[9]. However, single-filler systems tend to cause poor processability and mechanical properties of composites at a high level of filler content. Therefore, it has been a hot topic for introducing hybrid fillers with different dimensions into polymer matrices. Some researchers reported a hybrid filler of 2-dimensional (2-D) conductive network[10, 11], while others tried to fabricate 3-dimensional (3-D) pathway[12–17]. Moshe *et al.* found that the threshold percolation concentration for the polypropylene/glass fiber/carbon black (PP/GF/CB)-based materials occurs at about 1 wt% of CB, which is significantly lower than that for the reference CB-filled PP compounds[18], while in Cui *et al.*'s work[16], a synergistic effect of boron nitride (BN) with graphene nanosheets was observed on the enhancement of thermal conductive and mechanical properties of polymeric composites. In most of the works, the researchers tried to demonstrate a synergistic effect between different fillers, while in the system of hybrid fillers, the key point was the control of the filler network structure in a polymer matrix[19–22].

In terms of the polymer matrix, as one of the most important engineering plastics, nylon has been widely used in chemical industry. Poly(*m*-xylene adipamide) (MXD6) is a kind of crystalline aromatic nylon, with a series of advantages such as high distortion temperature, strength, resistance and barrier property[23–27]. It was reported that the oxygen barrier of MXD6 was five times greater than that of PA6, despite the fact that the crystallinity of MXD6 films was much lower than the latter[28].

Among various fillers, expanded graphite (EG) is regarded as one of the most economical and effective candidates for conductive enhancements due to its excellent electrical conductivity (5.9×10^7 S/m) and thermal conductivity (400 W/(m·K))[29–34]. On the other hand, carbon nanotubes (CNTs) have clearly demonstrated their capability as fillers in diverse multifunctional nanocomposites[31]. Because of their large aspect ratio and the sharp enhancement of electrical conductivity at very low percolation thresholds of CNTs in polymer matrix, it has been the highlight of fabricating polymer-based composites by adding CNTs[22, 35–37]. Thus in this study, the 2-dimensional (2-D) expanded graphite (EG) and the 1-dimensional (1-D) multi-walled carbon nanotubes (CNTs) were adopted as hybrid fillers. However, so far the majority of the researchers have emphasized the study about identifying the suitable filler content in which the optimum properties were observed, which otherwise is relatively monotonous. Therefore, in our study three types of filler contents representing different network morphology were systematically studied. In the first instance, EG was individually added into MXD6 to prepare the binary composites through melt blending to determine the percolation threshold. Then MXD6/EG composites with three compositions representing below percolation, just at percolation and above percolation, respectively, were chosen as a certain content of EG then melt-mixed with CNTs to make MXD6/EG/CNTs ternary composites. SEM and TEM were used to observe the morphology of the filler network.

With the systematic research on the composite properties at different filler contents, we propose a comprehensive evaluation mode in studying the relationship between macro-properties and micro-morphologies. Meanwhile, with the introduction of the nylon materials, we also provide guidance in industrial production of excellent engineering plastic composites with outstanding conductive properties.

EXPERIMENTAL

Materials

Nylon MXD6 (Grade S6001) was purchased from Mitsubishi Gas Chemical Company, Inc. Multi-wall carbon nanotubes (CNTs, NC7000, 1.5 μm in length, 9.5 nm in diameter) were purchased from Nanocyl S.A., Belgium. Low temperature expandable graphite, with the trade mark ADT KP801, was acquired from Shijiazhuang ADT Carbonic Material Factory (China).

Preparation of Expanded Graphite

EG was prepared by a rapid heat-treatment in a muffle furnace at 600 °C for 1 min thereby expanding to large flakes. Then it was smashed to relatively fine flakes with the average lateral size of ~150 μm at high speed by a functional grinder (BJ-100, 2.5×10^4 r/min) for 30 s.

Preparation of MXD6/EG/CNTs Composites

Melt-blending method was adopted to prepare the binary and ternary composites at 270 °C with 60 r/min for 10 min in an internal mixer. In the first step, EG was individually added into MXD6 to prepare the MXD6/EG binary composites to determine the percolation threshold. Then MXD6/EG composites with three compositions representing below percolation, just at percolation and above percolation, respectively, were chosen as fixed contents, and then mixed with varying contents of CNTs to prepare MXD6/EG/CNTs ternary composites. Nylon granules together with hybrid fillers were premixed by shaking for 10 s in a container to avoid aggregation of filler particles and then simultaneously added into mixer. All the materials were dehydrated in a vacuum drying oven at the temperature of 100 °C for 12 h before processing and moulding.

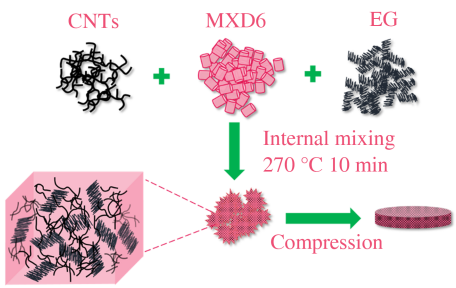

Fig. 1 Schematic diagram for the preparation of MXD6/EG/CNTs ternary composites

Characterization

The electrical conductivity of the samples, obtained by hot compression at 270 °C, with the average thickness of 2.6 mm, length of 30 mm and width of 5 mm was measured with a Keithley 6487 picoammeter under a constant voltage of 0.1 V in order to avoid strong electric current within the specimen. To prevent contact resistance, silver paint was brushed on both ends of the specimen with the brushed length being around 3 mm.

The transient place source (TPS) method was applied to measure the thermal conductivity of the samples by a Hot Disk thermal analyzer (Hot Disk 2500-OT, Uppsala, Sweden), based on which a disk-shaped sensor with the diameter of 2.005 mm was fixed between two round samples with the diameter of 15 mm and thickness of 2.6 mm. P2400 SiC paper was used in advance to smooth the samples' surfaces so as to achieve a good thermal contact.

Electromagnetic interference (EMI) shielding characteristics of the samples with the diameter of 13 mm and thickness of ~1.3 mm were tested through a coaxial test cell (APC-7 connector) connected with an Agilent N5230 vector network analyzer. The reflection loss (SE_R), absorption loss (SE_A) and total EMI shielding effectiveness (SE) (SE_T) were calculated using the equations:

$$SE_R = -10\lg(1-R) \tag{1}$$

$$SE_A = -10\lg\left(\frac{T}{1-R}\right) \tag{2}$$

$$SE_T = -10\lg T \tag{3}$$

$$R = 10^{(-0.1S_{11})} \tag{4}$$

$$T = 10^{(-0.1S_{21})} \tag{5}$$

where S_{ij} represents the power transmitted from port i to port j.

The cryo-fractured surfaces of MXD6/EG/CNTs, MXD6/EG and MXD6/CNTs composites were characterized to observe the morphology by using the scanning electron microscope (SEM, Inspect F, FEI Company, USA). The fractured surfaces were prepared in liquid N_2 for 2 h. Before observation, an ultrathin coating of gold was sputtered on the surface in vacuum. This was done to prevent the accumulation of static electric fields at the specimen due to the electron irradiation required during imaging. The morphology and dispersion status of EG and CNTs in MXD6 matrix were observed with transmission electron microscopy (TEM, JEF-2100F, JEOL) at an acceleration voltage 200 kV. Ultra-thin specimens were prepared at –90 °C using a Leica Ultra-thin UCT ultramicrotome with a knife made of diamond.

RESULTS AND DISCUSSION

Electrical Conductivity

The electrical conductivity (EC) of MXD6/EG and MXD6/CNTs binary composites was firstly investigated in order to determine the percolation threshold of each composite with single filler. A percolation phenomenon is usually observed as the filler content reaches to the threshold where a sharp increase of electrical conductivity is noticed[15]. Figure 2 depicts the curve of percolation in binary composites with single filler of either EG or CNTs loading. According to Fig. 2(a), one can estimate that the percolation threshold of binary composite lies around 0.2 wt% of CNTs loading and 10 wt% of EG loading, in which the electrical conductivity showed a sharp increase with more than four orders of magnitude and no further increase was observed after the critical filler content. After the determination of the percolation threshold for each binary system of MXD6/CNTs and MXD6/EG composites, the content of EG in the ternary MXD6/EG/CNTs composites was then chosen to be 5 wt% (below the percolation level), 10 wt% (just the percolation level) and 15 wt% (above the percolation level) respectively, and the CNTs' content changed from 0.5 wt% to 3 wt% so as to get a better understanding of the influence that different filler contents created on the improvement of the composites properties. A clear comparison in electrical conductivities of MXD6/EG binary and MXD6/EG/CNTs ternary composites with different hybrid filler contents can be seen from Fig. 2(b) that a small amount of CNTs added into MXD6/EG composites could lead to a jump in electrical conductivity, which is much higher than that of MXD6/EG composites with the same filler loading. Specifically, as for MXD6/10EG/*x*CNTs ternary composites, when the weight content of CNTs is 3 wt%, the electrical conductivity reaches 124.95 S/m, which is three orders of magnitude higher than that of binary composites at 13 wt% EG loading (0.2605 S/m).

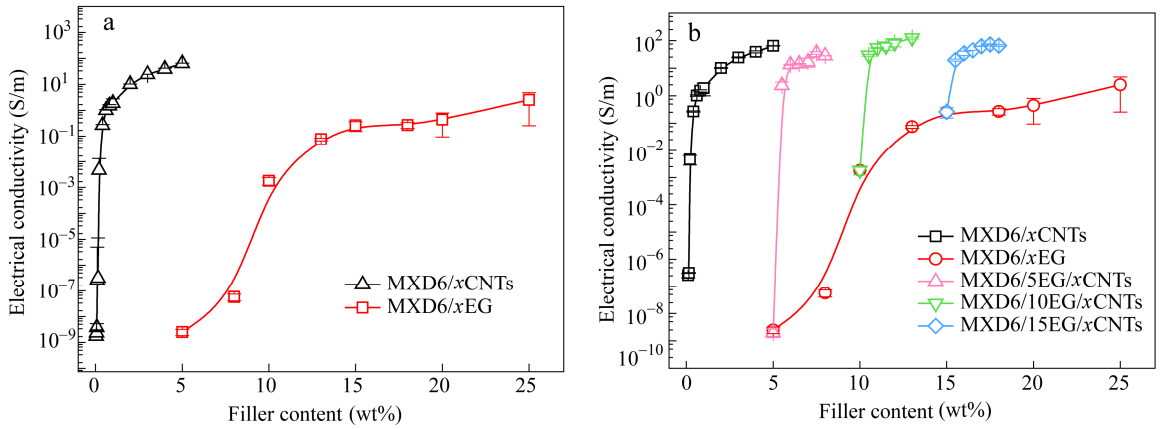

Fig. 2 Electrical conductivity of (a) MXD6/CNTs and MXD6/EG binary composites and (b) MXD6/EG/*x*CNTs ternary composites with increased filler content

The same result can be observed in the MXD6/5EG/3CNTs and MXD6/15EG/3CNTs systems, in which the electrical conductivities of ternary composites, with the values being 28.1 and 65.78 S/m, are much higher than those of MXD6/EG binary composites with the same filler loadings, namely 5.96×10^{-8} and

0.269 S/m, respectively. Therefore, with the aid of a small amount of CNTs, much less EG is required to obtain the conductive level, because CNTs embedding in the vacancy of EG layers could connect with each other and help to form an effective network in composites. Table 1 depicts an obvious comparison between binary and ternary composites with same filler loadings. It is worth noting that the electrical conductivity of MXD6/15EG/3CNTs composites is lower than that of MXD6/10EG/3CNTs. From such kind of trend, it can be explained that when EG content is beyond its percolation threshold, more CNTs could be trapped in the network of EG, as CNTs usually play a dominant role in the contribution of electrical conductivity. Thus they are more likely to be separated by EG layers, and then the paths for electron transmission in CNTs are impeded, resulting in a decreased electrical conductivity.

Table 1 Comparison of electrical conductivities between different ternary and binary composites with the same filler loadings

Filler content (wt%)	Electrical conductivity (S/m)
8EG	$5.69 \times 10^{-8} \pm 1.7 \times 10^{-8}$
5EG3CNTs	28.1 ± 0.13
13EG	0.0742 ± 0.0086
10EG3CNTs	124.95 ± 10.218
18EG	0.269 ± 0.0693
15EG3CNTs	65.78 ± 4.53

Thermal Conductivity

The thermal conductivities (TC) of the composites with single or hybrid fillers were then measured and compared with those of existing hybrid-filled composites according to Table 2 and Fig. 3. It can be seen from Fig. 3 that with the filler content increasing the thermal conductivity of composites exhibits a linearly rising trend for both binary and ternary composites. According to Fig. 3(a), pure MXD6 sample exhibits a relatively low thermal conductivity of 0.2494 W/(m·K), which could hardly meet the industrial demands[38]. Yet for binary composites of MXD6/CNTs, the increase of filler content does not lead to an obvious augmentation of the thermal conductivity, which ranges only from 0.2494 W/(m·K) to 0.4103 W/(m·K) and is just 64% higher than that of neat MXD6. But the presence of EG induces enhancement to the thermal conductivity of MXD6/EG composites and the enhancement greatly depends on the content of EG. For example, the thermal conductivity of MXD6/5EG binary composites is 0.423 W/(m·K), only 70% of the augmentation compared with neat MXD6 sample. But when the EG content reaches 25 wt%, the thermal conductivity is enhanced up to 3.762 W/(m·K), which is 1408.4% of increment. Thus it is apparent that the filler of EG plays a dominant role in enhancing the thermal conductivity of composites. As discussed earlier, we fix the large-sized EG content of 5 wt%, 10 wt% and 15 wt% respectively and change the small-sized CNTs content from 0.5 wt% to 3 wt%. As shown in Fig. 3(b), although no obvious percolation threshold is observed for the thermal conductivity, it increases linearly as the hybrid filler content is increased. For instance, the TC ranges from 0.5565 W/(m·K) to 0.728 W/(m·K) in MXD6/5EG/*x*CNTs composites, from 1.068 W/(m·K) to 1.438 W/(m·K) in MXD6/10EG/*x*CNTs composites, and from 1.522 W/(m·K) to 2.062 W/(m·K) in MXD6/15EG/*x*CNTs composites respectively. By observing the fitting lines in Fig. 3(b), it can be seen that in each ternary system, the slope increases with the increasing content of EG, which ranges from 0.09 of MXD6/5EG/*x*CNTs to 0.19 of MXD6/15EG/*x*CNTs. Such a direct proportion between the linear slope and EG content indicates that the addition of CNTs in binary composites with high content of EG could bring larger increasing rate in thermal conductivity compared with lower content of EG. This is because when the EG content is 5 wt%, which is below the percolation threshold, there exists plenty of large-sized vacancy between EG layers and the morphology is like “sea-island”; fillers are not contacting with each other, which results in insufficient paths for phonon transmission. However, for the EG content that is above the percolation threshold, the introduction of CNTs helps to form an abundant thermal conductive network in polymer matrix, by which more effective transmission of phonons can be realized.

Table 2 Comparison of the thermal conductivities of composites with hybrid fillers in some published papers

Matrix	Filler	Filler content (wt%)	Thermal conductivity (W/(m·K))	Ref.
PA6	Graphite	30	1.37	[39]
PA66	CF	20	0.48	[40]
PA6	CF	30	0.32	[41]
PA6	rGO	10	0.42	[13]
PA6	Graphene/BN	21.5	1.76	[16]
PA6	Graphite/CF	60	2.03	[42]
MXD6	EG/CNTs	18	2.06	This work

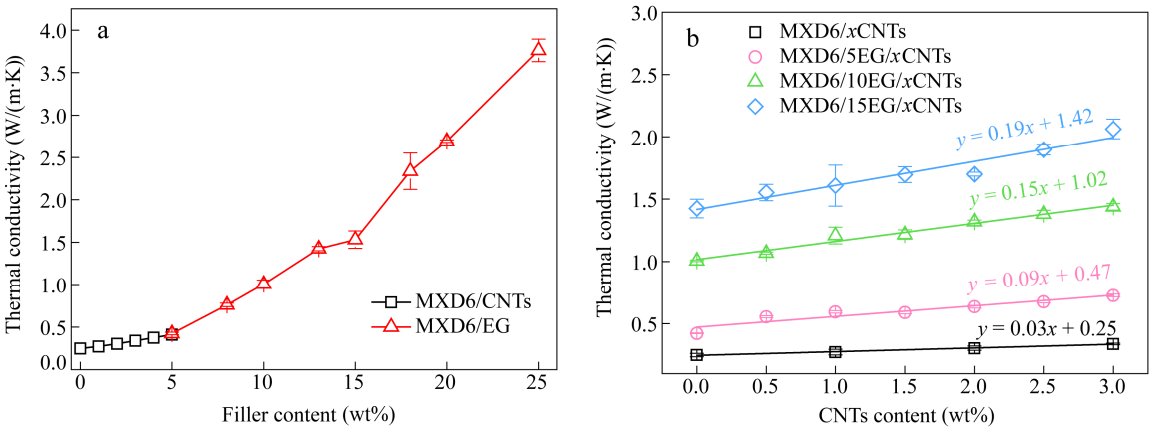

Fig. 3 Thermal conductivity of (a) MXD6/CNTs and MXD6/EG binary composites and (b) MXD6/EG/*x*CNTs ternary composites with increased filler content

Electromagnetic Interference Shielding Effectiveness

To further investigate the property of ternary composites with hybrid conductive fillers and explore their potential applications related to conductivity, the electromagnetic interference shielding effectiveness (EMI SE) of composites with different filler contents was then evaluated. It can be seen from Fig. 4 that in these three systems, the EMI SE is in direct proportion to the filler contents. From Figs. 4(a), 4(b) and 4(c), one can observe that the EMI value increases with the growing content of fillers, and the EMI values of MXD6/EG/CNTs ternary composites are much higher than those of the summation of MXD6/EG and MXD6/CNTs binary composites, which may be attributed to the synergistic effect between two conductive fillers. Specifically, when taking the EMI value under frequency of 10 GHz as an example, one can observe from Fig. 4(b) that the EMI value of MXD6/10EG is about 12 dB, and the value of MXD6/3CNTs is about 24 dB, while for ternary composites of MXD6/10EG/3CNTs the EMI value reaches up to around 45 dB, which is much higher than the summational value (36 dB) of two binary composites. This indicates that there exists obvious synergistic effect between two fillers in improving the EMI SE of ternary composites and the small-sized CNTs embedded in matrix fill in the vacancy of EG layers so that a more complete conductive network is formed by the combination of two different dimensional fillers. For composites with filler content of EG being 15 wt% and CNTs being 3 wt%, the EMI SE can reach as high as 50 dB, which is adequate to meet the application requirement[43], for it is estimated that materials with a shielding effectiveness greater than about 40 dB should be adequate for use in commercial applications[44]. Meanwhile, compared with neat MXD6 that shows a clear fluctuation at high frequency region (Figs. 4a, 4b and 4c), the electromagnetic shielding effect becomes more stable as the filler content increases. Figure 4(d) shows the comparison of the EMI SE among different EG loading composites at the fixed frequency of 10 GHz. The EMI value of ternary composites is around 30 dB at EG loading of 5 wt%, and it goes up to around 45 dB at 10 wt% EG level, which is 50% of the enhancement. This indicates that a conductive network inside composites is formed through adequate filler loading. In addition, by comparing the slopes of each fitting line, the increasing rates could then be clearly observed, in which the slope ranges from 7.56 in MXD6/5EG/*x*CNTs to 12.79 in MXD6/15EG/*x*CNTs. Obviously, this rising trend of slopes is just in consistence

with that in thermal conductivity, which once again proves the significance of high EG content in the property enhancement.

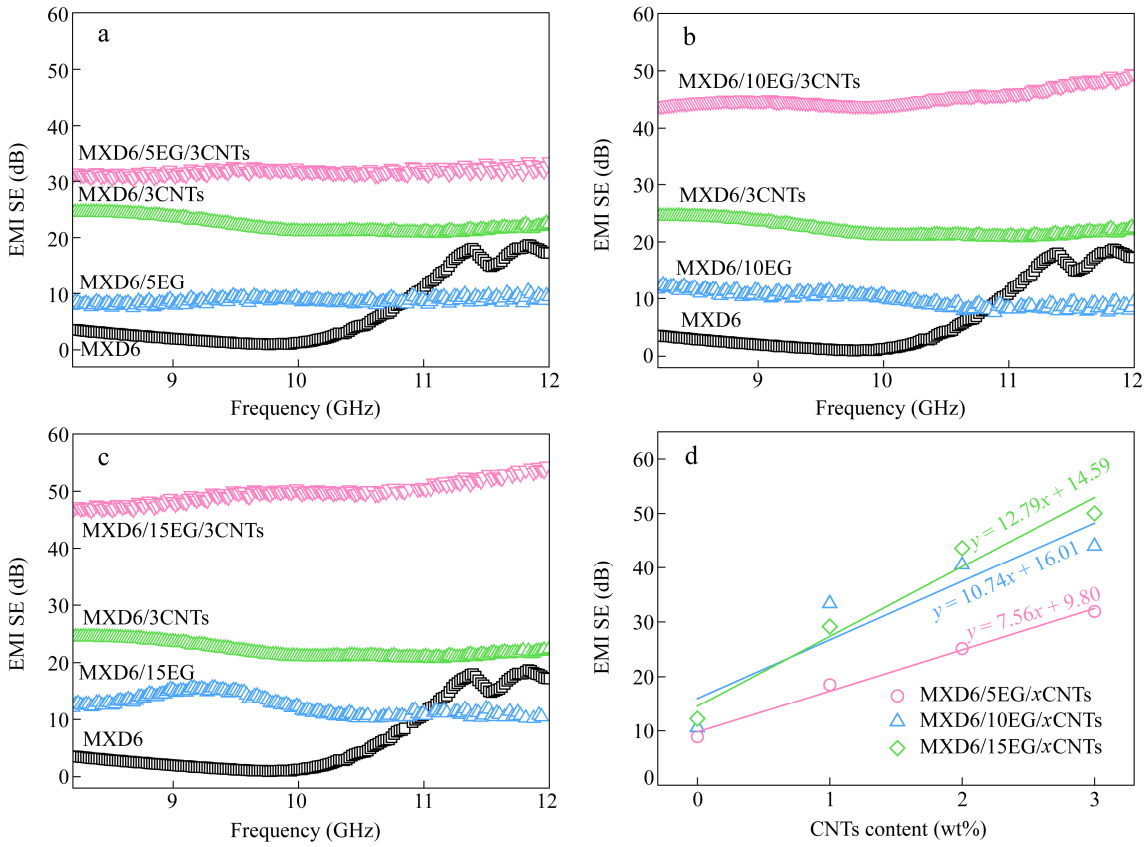

Fig. 4 Electromagnetic interference shielding effectiveness (EMI SE) of (a) MXD6/5EG/*x*CNTs, (b) MXD6/10EG/*x*CNTs, (c) MXD6/15EG/*x*CNTs ternary composites and (d) comparison of EMI SE in different systems under the certain frequency of 10 GHz with the increased CNTs content

The reflection loss and absorption loss as a function of CNTs concentration have then been investigated so as to quantify the contribution of different EMI shielding mechanisms to the total EMI SE. The key point to interpret the reflection and absorption mechanisms is the connectivity of fillers[35]. As shown in Fig. 5(a), the shielding by reflection increases with increasing filler content, which can be related to higher amount of mobile charge carriers. Unlike the shielding by reflection, according to Fig. 5(b), the shielding by absorption of MXD6/10EG/*x*CNTs reaches the highest among the three different systems, which indicates that the most effective connectivity of fillers occurs in 10 wt% of EG concentration and further increasing of the EG content may cause more thermal contact resistance in fillers, which would hinder the shielding by absorption as a result.

Distribution of Conductive Fillers

The morphology of composites helps to understand the distribution of two conductive fillers, and hence scanning electron microscopy was utilized. The uniform dispersion of fillers and the strong interfacial adhesion can significantly affect the performance of polymer composites[45]. For binary composites with either EG or CNTs loaded in polymer matrix, as observed in Fig. 6, single filler could not form adequate effective networks due to either less contact or aggregation among fillers, which hinders the transmission of phonons and electrons. Especially for MXD6/CNTs system, there exists strong π-π interaction between CNTs thus it shows an agglomerated state which is hard to be spread during processing. And the addition of large-sized EG could

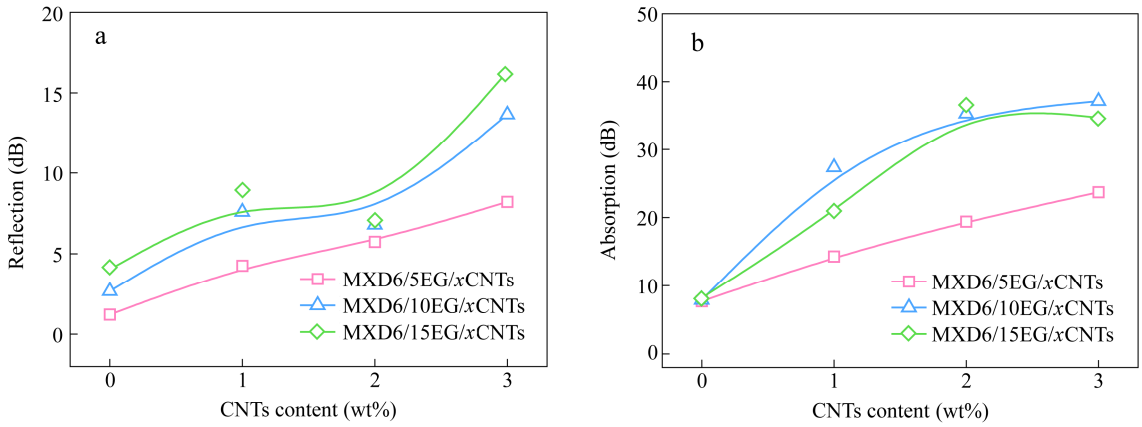

Fig. 5 Contributions of (a) reflection and (b) absorption to the overall EMI SE for samples as a function of CNTs concentration

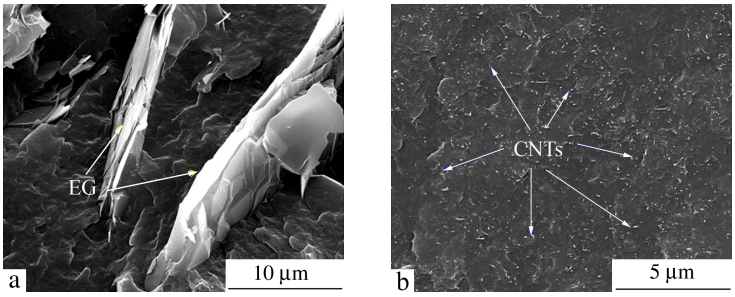

Fig. 6 SEM images of the dispersion and morphology of fillers in (a) MXD6/EG and (b) MXD6/CNTs binary composites at different magnifications

promote the homogeneous dispersion of CNTs. Figure 7 depicts the fracture morphology of composites with different hybrid filler contents with EG being 5 wt%, 10 wt% and 15 wt% respectively. It can be seen from Figs. 7(a), 7(b) and 7(c) that those light sticks distributed in matrix are EG layers, and they present a relatively homogeneous distribution in nylon matrix and the distribution becomes denser with more filler loading. It can be seen from Fig. 7(c2) at high magnification that CNTs, observed as little white dots, are evenly distributed among layers of EG, and they act like bridges to connect fillers together so as to form effective pathways for the heat and electrical flow along CNTs. Such dispersion of fillers could be more clearly observed from TEM images. As can be seen from Fig. 8, it is obvious that there exists vacancy between the layers of large-sized EG and then the small-sized CNTs filling into that vacancy contact with each other so that the loosed EG layers have been linked together by the dense CNTs.

On the other hand, the conductive mechanisms drawn as follows help to understand the change in conductive network caused by different contents of expanded graphite. As can be seen from Fig. 9(a), when the EG content is 5 wt%, the morphologies are similar to “isolated islands” between fillers and “sea-island” between fillers and matrix. The layers between EG and CNTs are separated, where too many large-sized vacancies between EG layers exist. In that case, fillers are hard to contact with each other and the morphology exhibits a non-network situation at this filler level, which could lead to a poor transmission for both electrons and phonons among EG sheets and a poor shielding for electromagnetic waves. So it presents a low electrical and thermal conductivity at the macroscopic level, which is defined as below-percolation. From Fig. 9(b), it is evidenced that when 10 wt% of EG is achieved, fillers are just connected with each other effectively, with no other redundant contact resistance. And the 1-D CNTs, in contact with each other, could serve as bridges among the layers of 2-D EG and form a dense network in these vacancies. Then an efficient conductive network is constructed by hybrid fillers with the synergistic effect. Therefore the effectiveness of composites at that filler content level

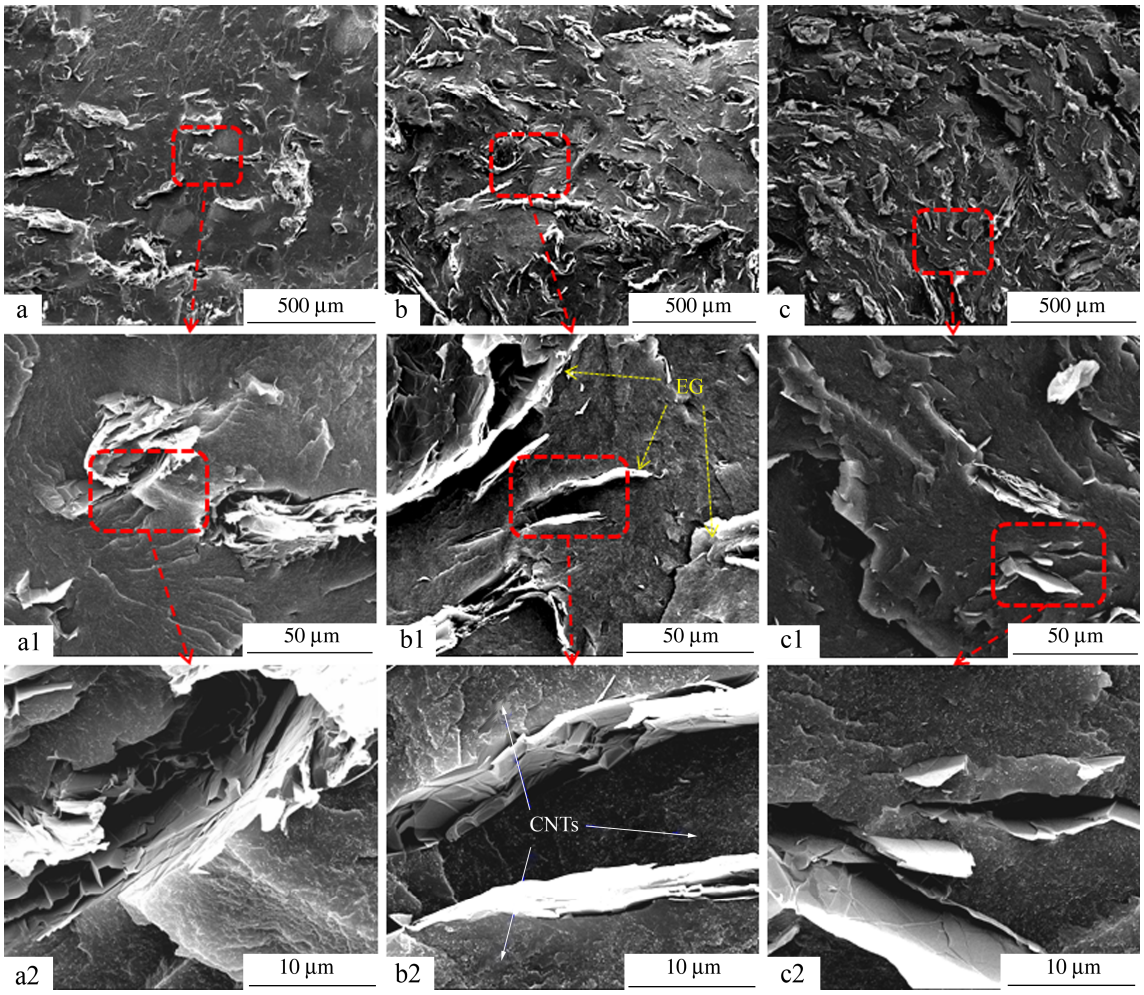

Fig. 7 SEM images of the dispersion and morphology of fillers in (a) MXD6/5EG/3CNTs, (b) MXD6/10EG/3CNTs and (c) MXD6/15EG/3CNTs ternary composites with increased magnification

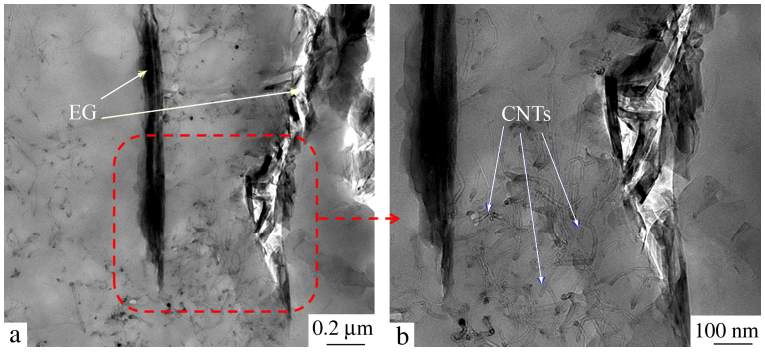

Fig. 8 TEM images of the dispersion and morphology of fillers in MXD6/10EG/3CNTs ternary composites with (a) low and (b) high magnification

reaches the optimum properties on macroscopic scale, which is regarded as just- percolation filler loading. However with further increasing the filler content to 15 wt%, as defined as above percolation, shown in Fig. 9(c), EG and CNTs are fully contacted with each other and not much more vacancies could be seen. In that occasion, the density of the filler network is the dominant factor, and the vacancies are all fixed. The small-sized

CNTs are even separated by plenty of large-sized EG layers, so the enhancement of electrical conductivity at the filler loading shows a slight decrease.

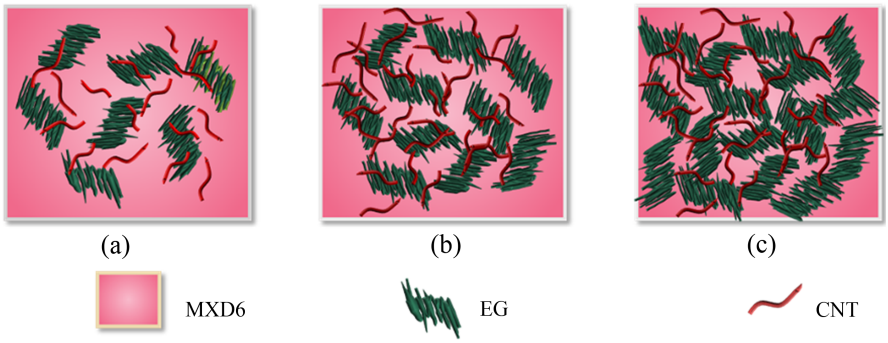

Fig. 9 Schematic representations showing the morphological changes of fillers in ternary composites in the EG state of (a) below (5 wt%), (b) just (10 wt%) and (c) above (15 wt%) the percolation threshold

CONCLUSIONS

Above all, by adoption of different dimensional fillers in polymer matrix, we successfully fabricated nylon-based composites with excellent properties in electrical conductivity, thermal conductivity and electromagnetic interference shielding effectiveness. The characteristic methods showed that the significant improvements of the EC, TC and EMI SE could be attributed to the synergistic effect between two fillers and the outstanding interaction between polymer matrix and fillers. On the other hand, by comparing different mass fractions of single fillers of below, just and above the percolation threshold, it can be concluded that the composites present the best properties when the filler content is just around the percolation threshold, where fillers just contact with each other and construct a most effective conductive path. And further addition of fillers makes little contribution to the enhancement of the properties due to fixed vacancies among filler layers.

REFERENCES

1 Levy, S., "Electromagnetic shielding effect of an infinite plane conducting sheet placed between circular coaxial coils", Institute of Radio Engineers, 1936, p. 923
2 Ji, K.J., Zhao, H.H., Zhang, J., Chen, J. and Dai, Z.D., Appl. Surf. Sci., 2014, 311: 351
3 He, Y.L., Guo, Y.L., He, R., Jin, T.X., Chen, F., Fu, Q., Zhou, N. and Shen, J., Chinese J. Polym. Sci., 2015, 33(8): 1176
4 Su, B., Zhao, Y.S., Chen, F. and Fu, Q., Chinese J. Polym. Sci., 2015, 33(7): 964
5 Deng, S., Qi, X.D., Zhu, Y.L., Zhou, H.J., Chen, F. and Fu, Q., Chinese J. Polym. Sci., 2016, 34(10): 1270
6 Rosato, D.V., "Plastics processing data handbook", Springer Science & Business Media, 2012, p. 32
7 Zhang, K., Chai, Y., Yuen, M., Xiao, D. and Chan, P., IOP science, 2008, 19: 1
8 Zeng, X.P., Yang, J.J. and Yuan, W.X., Eur. Polym. J., 2012, 48(10): 1674
9 Tu, W.Y., Zhang, H.Y., Hong, H.Q. and Zhang, X.B., Plastics, 2012, 41(5): 73
10 Chen, J., Du, X.C., Zhang, W.B., Yang, J.H., Zhang, N., Huang, T. and Wang, Y., Compos. Sci. Technol., 2013, 81: 1
11 Cui, C.H., Yan, D.X., Pang, H., Jia, L.C., Bao, Y., Jiang, X. and Li, Z.M., Chinese J. Polym. Sci., 2016, 34(12): 1490
12 Im, H. and Kim, J., Carbon, 2012, 50(15): 5429.
13 Xiao, Y.J., Wang, W.Y., Lin, T., Chen, X.J., Zhang, Y.T., Yang, J.H., Wang, Y. and Zhou, Z.W., J. Phys. Chem. C, 2016, 120(12): 6344
14 Zhang, W.B., Zhang, Z.X., Yang, J.H., Huang, T., Zhang, N., Zheng, X.T., Wang, Y. and Zhou, Z.W., Carbon, 2015, 90: 242
15 Wu, K., Xue, Y., Yang, W.X., Chai, S.G., Chen, F. and Fu, Q., Compos. Sci. Technol. 2016, 130: 28

16 Cui, X.L., Ding, P., Zhuang, N., Shi, L.Y., Song, N. and Tang, S.F., ACS Appl. Mater. Interfaces, 2015, 7(34): 19068
17 Celzard, A., Mareche, J. and Furdin, G., Prog. Mater. Sci., 2005, 50(1): 93
18 Moshe, N., Gershon, L., Anita, V. and Limor, Z., J. Electrostat., 1999, 47: 201
19 Deng, H., Skipa, T., Bilotti, E., Zhang, R., Lellinger, D., Mezzo, L., Fu, Q., Alig, I. and Peijs, T., Adv. Funct. Mater., 2010, 20(9): 1424
20 Rohini, R. and Bose, S., ACS Appl. Mater. Interfaces, 2014, 6(14): 11302
21 Maiti, S., Shrivastava, N.K., Suin, S. and Khatua, B.B., ACS Appl. Mater. Interfaces, 2013, 5(11): 4712
22 Yang, K. and Gu, M.Y., Compos. Part A-Appl. S., 2010, 41(2): 215
23 Tang, J.W., Wu, F. and Li, M.Y., Plastic Packaging, 2008, 18(2): 47
24 Wang, Y.Q., Modern Plastics Processing and Applications, 1997, 9(3): 43
25 Thellen, C., Schirmer, S., Ratto, J.A., Finnigan, B. and Schmidt, D., J. Membr. Sci., 2009, 340(1-2): 45
26 Bao, Z.B., Wang, J., Pan, J. and Xu, W.B., Engineering Plastics Application, 2013, 41(4): 67
27 Zhang, B.Y., Ge, Q.S., Guo, Z.X. and Yu, J., Chinese J. Polym. Sci., 2016, 34(8): 1032
28 Fereydoon, M., Tabatabaei, H.S. and Ajji, A., Macromolecules, 2014, 47(7): 2384
29 Working, D.C., Connell, J.W., Smith, J.J.G., Watson, K.A., Delozier, D.M., Sun, Y.P. and Lin, Y., High Perform. Polym., 2006, 961
30 Kalaitzidou, K., Fukushima, H., Askeland, P. and Drzal, L.T., J. Mater. Sci., 2007, 43(8): 2895
31 Balandin, A.A., "Thermal Properties of Graphene, Carbon Nanotubes and Nanostructured Carbon Materials", Thesis, University of California, 2011
32 Yu, A.P., Ramesh, P., Itkis, M.E., Bekyarova, E. and Haddon, R.C., J. Phys. Chem. C, 2007, 111: 7565
33 Fukushima, H., Drzal, L.T., Rook, B.P. and Rich, M.J., J. Therm. Anal. Calorim., 2006, 85: 235
34 Veca, L.M., Meziani, M.J., Wang, W., Wang, X., Lu, F.S., Zhang, P.Y., Lin, Y., Fee, R., Connell, J.W. and Sun, Y.P., Adv. Mater., 2009, 21(20): 2088
35 Arjmand, M., Apperley, T., Okoniewski, M. and Sundararaj, U., Carbon, 2012, 50(14): 5126
36 Ayesha, K., Chinese J. Polym. Sci., 2013, 32(1): 64
37 Bao, H.D., Guo, Z.X. and Yu, J., Chinese J. Polym. Sci., 2009, 27(3): 393
38 Zhang, K., Chai, Y., Yuen, M.M., Xiao, D.G. and Chan, P.C., Nanotechnology, 2008, 19(21): 215706
39 Zhou, S.T., Chen, Y., Zou, H.W. and Liang, M., Thermochim. Acta, 2013, 566: 84
40 Heiser, J.A. and King, J.A., Polym. Compos., 2004, 25(2): 186
41 Yan, X.L., Imai, Y., Shimamoto, D. and Hotta, Y., Polymer, 2014, 55(23): 6186
42 Yoo, Y., Lee, H.L., Ha, S.M., Jeon, B.K., Won, J.C. and Lee, S.G., Polym. Int., 2014, 63(1): 151
43 Joo, J. and Epstein, A.J., Appl. Phys. Lett., 1994, 65(18): 2278
44 Colaneri, N.F. and Shacklette, L.W., IEEE T Instrum. Meas., 1992, 41: 291
45 Geng, C.Z., Hu, X., Yang, G.H., Zhang, Q., Chen, F. and Fu, Q., Chinese J. Polym. Sci., 2014, 33(1): 61